Hindawi Publishing Corporation
Journal of Nanomaterials
Volume 2016, Article ID 7589028, 9 pages
http://dx.doi.org/10.1155/2016/7589028

Research Article

Fabrication of Cubic p-n Heterojunction-Like NiO/In_2O_3 Composite Microparticles and Their Enhanced Gas Sensing Characteristics

Hou Xuemei,[1,2] Sun Yukun,[3] and Bai Bo[3]

[1]*School of Information Engineering, Chang'an University, Xi'an 710054, China*
[2]*Department of Intelligent Science and Technology, Xi'an University of Posts and Telecommunications, Xi'an 710121, China*
[3]*Key Laboratory of Subsurface Hydrology and Ecological Effects in Arid Region (Chang'an University), Ministry of Education, Xi'an 710054, China*

Correspondence should be addressed to Bai Bo; baibochina@163.com

Received 20 October 2016; Accepted 29 November 2016

Academic Editor: Xiulin Fan

Oxide semiconductor In_2O_3 has been extensively used as a gas sensing material for the detection of various toxic gases. However, the pure In_2O_3 sensor is always suffering from its low sensitivity. In the present study, a dramatic enhancement of sensing characteristic of cubic In_2O_3 was achieved by deliberately fabricating p-n heterojunction-like NiO/In_2O_3 composite microparticles as sensor material. The NiO-decorated In_2O_3 p-n heterojunction-like sensors were prepared through the hydrothermal transformation method. The as-synthesized products were characterized using SEM-EDS, XRD, and FT-IR, and their gas sensing characteristics were investigated by detecting the gas response. The experimental results showed that the response of the NiO/In_2O_3 sensors to 600 ppm methanal was 85.5 at 260°C, revealing a dramatic enhancement over the pure In_2O_3 cubes (21.1 at 260°C). Further, a selective detection of methanol with inappreciable cross-response to other gases, like formaldehyde, benzene, methylbenzene, trichloromethane, ethanol, and ammonia, was achieved. The cause for the enhanced gas response was discussed in detailed. In view of the facile method of fabrication of such composite sensors and the superior gas response performance of samples, the cubic p-n heterojunction-like NiO/In_2O_3 sensors present to be a promising and viable strategy for the detection of indoor air pollution.

1. Introduction

In the past years, indoor air pollution has been realized by many people with respect to public health. Methanal, as typical air pollution indoor, is seriously toxic to human beings and animals even at very low concentration [1]. As a result, the strategies to effectively detect low concentration methanol are of great significance and in huge demand in practical applications. Currently the most commonly used technologies for detecting the low concentration methanal in air include fluorimetry [2], colorimetry [3], high-performance liquid chromatography (HPLC) [4], gas chromatography (GC) [5], and infrared detection [6]. In contrast to such traditionally available approaches for detecting methanal, another alternative monitor using oxide semiconductor as sensor has been recently applied due to its various superiorities, such as low cost, good stability, and short response time [7–10]. Typically, a series of oxide semiconductor-based gas sensors, like SnO_2 [11], TiO_2 [12], In_2O_3 [13], and Fe_2O_3 [14], have been reported to act as gas sensors for detecting methanal.

Presence of space charge layers in semiconductors is a common phenomenon within a heterojunction structure once two semiconductor materials with different band gaps are intimately contacted [15]. In such formed heterojunction layer, free electrons in one material with higher Fermi energy could migrate into the adjacent material spontaneously due to the demand of band alignment until their Fermi levels allied at the same energy, resulting in the opposite charges at two sides of heterostructure interface. In a word, a unique space charge layer, which contains opposite charges within the different semiconductor component, is apt to be generated [16]. More specifically, in n-type oxide semiconductors, the

adsorption of electronegative oxygen generates an electron depletion layer near the semiconductors surface. Thereby, sensor resistance is rest with the close-knit connection between the resistive electron depletion layer and semiconducting cores. In p-type oxide semiconductors, the ionized adsorption of oxygen can create the hole accumulation layer through electrostatic interaction between positively charged holes and negatively charged oxygen. In such interaction circumstances, the sensor resistance strongly depends on the competition of conduction along the cabined cross-sectional area of hole accumulation layer near-surface and that across resistive cores with a wide cross-sectional area [17, 18]. In contrast, the gas response of n-type oxide semiconductors is often relatively higher than that of p-type oxide semiconductors because of the imparity in their gas sensing mechanisms [19]. However, p-type oxide semiconductors are ideally suitable for the designing of novel functionality in high-performance gas sensors, since they own a distinctive catalytic activity with multifarious volatile organic compounds [20]. By this token, the combination of n-type oxide semiconductors with p-type oxide semiconductors to design a novel hybrid or composite semiconductor material is attracting increasing attention as it enables new functional properties, which are not possible in their own starting components. Typically, some admirable candidates have been offered currently by the heterostructured formation of oxide-oxide p-n junctions, improving functional properties in comparison with the pure parent substrate. For instance, p-n heterojunction-like ZnO/TiO_2 [21], WO_3/TiO_2 [22], NiO/TiO_2 [23], $CuBi_2O_4/TiO_2$ [24], and In_2O_3/ZnO [25] have been synthesized triumphantly.

In_2O_3, a classical n-type III–V semiconductor with a wide band gap (3.6 eV), displays a predominant sensing performance towards a broad category of gases, such as H_2S [26], CO [27], C_3H_6O [28], and C_2H_5OH [29]. Hence, In_2O_3-based sensors show an efficient sensing performance in different conditions. For example, Sun et al. pointed out that In_2O_3 was a highly sensing material for the detection of various gases, and the adding of palladium and platinum was proved to be a simple and efficient route to enhance the sensing properties [30]. Wang and coworkers reported the Er-doped In_2O_3 nanotube, and the response of the Er-doped In_2O_3 nanotube sensors to 20 ppm methanal was 12 at 260°C in the subsequent gas sensing investigation, which was very promising for the detection of dilute methanal gas in practice [31]. NiO has been widely used in sensors [32], antiferromagnetic devices [33], fuel cells [34], and dye-sensitized photocathodes [35] due to its simple structure, electrochemical stability, high durability, and low cost. As a typical p-type semiconductor, NiO is also a benign candidate to design the new functionality in high-performance gas sensors. For instance, Ju et al. reported NiO/SnO_2 p–n junction which was formed by depositing NiO nanoparticles onto the surface of SnO_2 hollow sphere sensors, and the response of NiO/SnO_2 sensor was much higher than that of pristine SnO_2 hollow spheres [36]. Li and coworkers have synthesized the p-NiO/n-ZnO nanowire heterojunction structure for the applications in UV sensors [37]. In comparison with the great success above-mentioned, the design of high-performance NiO/In_2O_3 oxide-oxide semiconductor gas sensors with p-n heterojunction-like structure is still very much in the early stages of investigation. Particularly, no one has reported the synthesis and gas sensing performance of cubic NiO/In_2O_3 composites with NiO as loaded material.

Based on the above background, in the present study p-n heterojunction-like NiO/In_2O_3 microparticles were prepared through a hydrothermal synthesis method. The as-synthesized product was characterized using SEM-EDS, XRD, and FT-IR. Then, a comparative gas sensing study was performed to illuminate the conspicuous sensing properties of the NiO/In_2O_3 sensors. The experimental results demonstrated that a dramatic enhancement of sensing characteristic of cubic In_2O_3 has been achieved in comparison with the single In_2O_3 materials, and the cause for the improvement of gas sensing property to methanal can be assigned to the deliberate surface ornament of cubic In_2O_3 substrate with petal-shaped NiO nanoparticles. In view of the facile method of fabrication of the composite sensors and the superior gas response performance, we believed that the p-n heterojunction-like NiO/In_2O_3 sensors present to be a promising and viable strategy for the detection of indoor methanal pollution.

2. Experimental

2.1. Synthesis of NiO/In_2O_3. Originally, the $In(OH)_3$ and $Ni(OH)_2$ were prepared by a hydrothermal reaction process. In detail, a spot of $InCl_3$ was firstly dissolved in 100 mL distilled water under vigorous stirring at room temperature. Then, the moderate sodium dodecyl benzene sulfonate (SDBS) was added to the solution. Next, the mixture was transferred to a teflon-lined stainless steel autoclave, sealed, and maintained at 473.15 K for 24.0 h. The autoclave was allowed to cool down to room temperature naturally. The resulting white precipitate ($In(OH)_3$) was filtered and washed with distilled water. For the $Ni(OH)_2$, solid $NiCl_2$ was firstly dissolved in 160 mL distilled water, and the urea was added to the solution under vigorous stirring. The mixture was transferred to the stainless steel autoclave, sealed, and maintained at 473.15 K for 24.0 h. The green precipitate ($Ni(OH)_2$) was obtained. Secondly, the preparation of $Ni(OH)_2/In(OH)_3$ compound was conducted in the stainless steel autoclave. The as-prepared $In(OH)_3$ was added to the saturated $NiCl_2$ solution, followed by the 5.0 h hydrothermal reaction at 473.15 K. The laurel-green compound $Ni(OH)_2/In(OH)_3$ was filtered and washed with distilled water. Ultimately, $Ni(OH)_2/In(OH)_3$ composites were placed in crucible and heat-treated for 1.0 h at 873.15 K to yield yellow-green solid NiO/In_2O_3 products.

2.2. Characterization of the Samples. The p-n heterojunction-like NiO/In_2O_3 microparticles were characterized by scanning electron microscopy (SEM, Hitachi S-4800) and X-ray diffraction (XRD, Rigaku D/MAX-3C diffract meter). Fourier-transform infrared (FT-IR) spectra of materials were performed on a Bio-Rad FTS135 spectrometer using a KBr wafer technique.

2.3. Gas Sensor Fabrication and Response Test. Firstly, In_2O_3 and NiO/In_2O_3 slurries were formed by dispersing them in

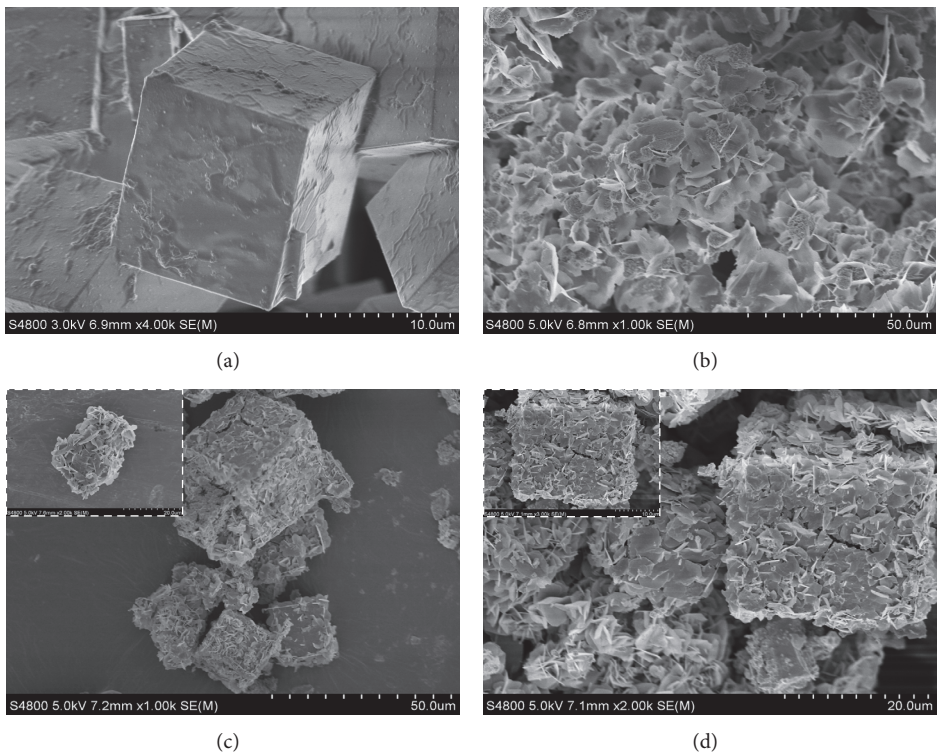

Figure 1: SEM images of (a) $In(OH)_3$, (b) $Ni(OH)_2$, (c) $Ni(OH)_2/In(OH)_3$, and (d) p-NiO/n-In_2O_3.

deionized water. Then, the as-prepared In_2O_3 and NiO/In_2O_3 slurries were directly drop-coated on the outer surface of alumina substrates with two Au electrodes. After drying for approximately 3.0 h at 60°C, the sensors were annealed subsequently at 600°C for another 3.0 h. To guarantee the long-term stability, aging test for 2 days was carried out to the sensors.

For the measurement system (WS-30A), the gas response R of the sensor can be calculated by the equation: $R = R_g/R_a$ (where R_g is resistance in gas and R_a is resistance in air). The gas responses to formaldehyde (HCHO), benzene (C_6H_6), methylbenzene ($C_6H_5CH_3$), trichloromethane ($CHCl_3$), ethanol (C_2H_5OH), and ammonia (NH_3) were measured. In addition, the gas concentrations were also studied. The substrate temperature was adjusted between 220°C and 320°C by controlling the heater powers.

3. Results and Discussion

3.1. Structure and Morphology. Figure 1 shows the SEM pictures of the (a) $In(OH)_3$, (b) $Ni(OH)_2$, (c) $Ni(OH)_2/In(OH)_3$, and (d) p-NiO/n-In_2O_3. As can be seen in Figure 1(a), the $In(OH)_3$ precursors have an ordered cubic structure with size of ~10 μm, and the $In(OH)_3$ microparticles also have a relative smooth surface. In Figure 1(b), the parallel samples of $Ni(OH)_2$ nanoparticles possessed a uniform petal-shaped morphology with very good dispersibility. After decorating the cubic $In(OH)_3$ precursors with $Ni(OH)_2$ nanoparticles, it can be seen in Figure 1(c) that almost each of cubic $In(OH)_3$ microparticles was surrounded by petal-shaped $Ni(OH)_2$ nanoparticles, forming the precast complex structure. After the calcination of $Ni(OH)_2/In(OH)_3$ for 24.0 h, the p-n heterojunction-like NiO/In_2O_3 microparticles were prepared. As seen in Figure 1(d), calcining process did not influence seriously the morphology of $Ni(OH)_2/In(OH)_3$; therefore, the cubic In_2O_3 and petal-shaped NiO were observed. Compared to the smooth surface of original $In(OH)_3$ precursors, the synthetic p-NiO/n-In_2O_3 have been altered to the rough surface structure (inset in Figure 1(d)). In structure, the gas sensing properties always strongly relied on their surface properties and shapes of the composites, and the p-NiO/n-In_2O_3 oxide semiconductor microparticles met the requirement of great surface-to-volume ratios. Moreover, in favor of the gas sensing characteristics, NiO maintained the excellent dispersibility, other than agglomerating together.

XRD spectra of the as-prepared (a) $In(OH)_3$, (b) $Ni(OH)_2$, (c) $Ni(OH)_2/In(OH)_3$, and (d) p-NiO/n-In_2O_3 composite particles are exhibited in Figure 2. In Figure 2(a), the $In(OH)_3$ cubes were well crystallized, which could be corroborated by the JCPDS 16-161. Namely, all the peaks of Figure 2(a) could be indexed to a pure body centered cubic phase of $In(OH)_3$. In Figure 2(b), almost all the reflections of the $Ni(OH)_2$ could be readily indexed to a hexagonal phase (JCPDS number 14-0117), and no other characteristic peaks were detected for impurities. After the loading of $Ni(OH)_2$, the precursor compounds $Ni(OH)_2/In(OH)_3$ demonstrated the XRD patterns both of $Ni(OH)_2$ and $In(OH)_3$, which in turn offered the evidence of the resultant compounds $Ni(OH)_2/In(OH)_3$. The resultant $Ni(OH)_2/In(OH)_3$ compounds contain the typical peaks of $Ni(OH)_2$ and $In(OH)_3$,

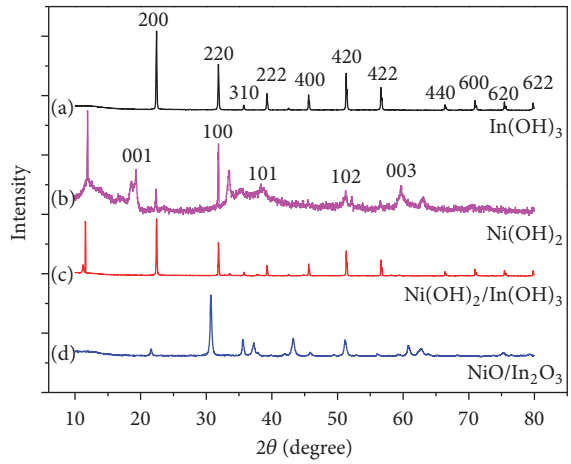

Figure 2: XRD patterns of (a) $In(OH)_3$, (b) $Ni(OH)_2$, (c) $Ni(OH)_2/In(OH)_3$, and (d) p-NiO/n-In_2O_3.

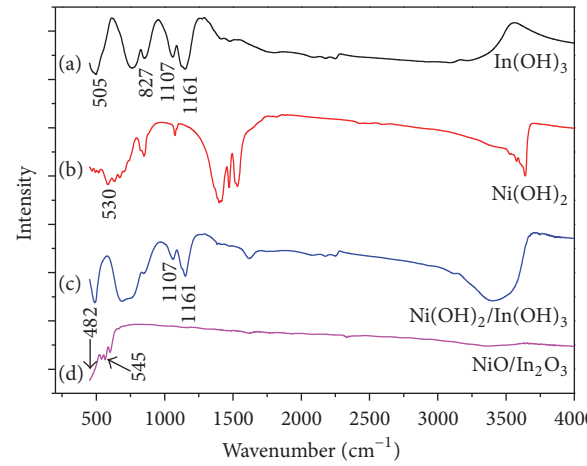

Figure 3: FT-IR spectra of (a) $In(OH)_3$, (b) $Ni(OH)_2$, (c) $Ni(OH)_2/In(OH)_3$, and (d) p-NiO/n-In_2O_3.

implying the presence of both $Ni(OH)_2$ and $In(OH)_3$. The final products p-NiO/n-In_2O_3 are displayed in Figure 2(d). It should be noted that not only the patterns of NiO (JCPDS number 44-1159) but also the peaks of In_2O_3 (JCPDS number 06-0416) appeared, suggesting the successful synthesis of the final NiO/In_2O_3 products.

To confirm the interaction between p-NiO and n-In_2O_3 during the formation of gas sensors composites, FT-IR spectroscopy was employed to monitor the chemical bond transformation of parallel precursor and p-n heterojunction-like NiO/In_2O_3 materials. Figure 3(a) depicts the FT-IR spectrum of $In(OH)_3$. The strong and broad bands at 3425 cm^{-1} (O-H stretching vibrations), 827 cm^{-1} (O-H bending vibration), 1161 cm^{-1}, and 1107 cm^{-1} and 505 cm^{-1} (In-OH absorption bands) were the characteristic absorption peaks of the native $In(OH)_3$. In Figure 3(b) of $Ni(OH)_2$, the peak at 3642-3424 (O-H stretching vibrations), a broad band at 1637 cm^{-1} which belongs to the bending vibration of absorbed water, and the peak at 530 cm^{-1} (Ni-OH bending vibration) were presented [38–40]. In the spectrum of $Ni(OH)_2/In(OH)_3$ in Figure 3(c), the bands at 530-505 cm^{-1} (Ni-OH) and 1161 cm^{-1} and 1107 cm^{-1} (In-OH) appeared simultaneously, implying that $Ni(OH)_2$ has been attached to the surface of $In(OH)_3$. After the thermal transition from $Ni(OH)_2/In(OH)_3$ to p-NiO/n-In_2O_3, p-NiO/n-In_2O_3 spectrum is shown in Figure 3(d). As we can see, the characteristic peaks at 482 cm^{-1} and 545, 488 cm^{-1} belong to the stretching vibrations of Ni-O and In-O-In, respectively. In combination with the analysis of above-mentioned SEM and XRD, we can confirm that NiO was firmly assembled onto the surface of the In_2O_3.

On the basis of SEM, XRD, and FT-IR, a possible formation mechanism of NiO/In_2O_3 microparticles was proposed: the $In(OH)_3$ solid powder was put in the saturated $NiCl_2$ solution in advance. Then, the OH^- from $In(OH)_3$ react with Ni^{2+} in the solution, generating the insoluble $Ni(OH)_2$ and replacing segmental indium ion. During this process, the Oswald ripening in the initial formation of $Ni(OH)_2$ occurred due to the rapid spread of nickel ion. As to a certain size of $Ni(OH)_2$, the Oswald ripening was ceased because the atomic exchange of Ni^+ cannot reduce the total interfacial energy. Therefore, $Ni(OH)_2$ could germinate on the surface of $In(OH)_3$, forming the $Ni(OH)_2/In(OH)_3$ composites. Along with the increase of reaction time, the loading of $Ni(OH)_2$ increased on the surface of $In(OH)_3$. Obviously, the rich surface hydroxyl of $In(OH)_3$ has served as active site for the surface modification process through a condensation reaction with the hydroxyl of $Ni(OH)_2$. In the meantime, the thus-treated particles were also coated by the SDBS molecule, which has an appropriate alkyl chains to stabilize these tiny nanocrystals and keep the particles from agglomerating. In another word, the spontaneous agglomerations in the reactor have been avoided by the use of SDBS molecule to reduce the surface activity of nanoparticles through the surface modification process. Thus, $Ni(OH)_2/In(OH)_3$ composite particles with a comparatively smaller diameter and a narrower size distribution could be generated. After calcination, the final product of NiO/In_2O_3 compound was obtained.

3.2. Gas Sensing Properties of the p-n Heterojunction-Like NiO/In_2O_3 Microparticles. The dynamic sensing transients of sensors (pure In_2O_3, NiO/In_2O_3 by hydrothermal reaction for 3.0 h and NiO/In_2O_3 by hydrothermal reaction for 24.0 h) to 600 ppm methanal gas were measured at 260°C (in Figure 4). As we can see in Figure 4, a pure In_2O_3 sensor displayed the lowest response. However, such low response could be slightly increased by NiO/In_2O_3 for hydrothermal reaction of 3.0 h. Further, the gas response value of the NiO/In_2O_3 sensors by hydrothermal reaction for 24.0 h was 85.55, which was almost four times more than pure In_2O_3. The gas response of the 24.0 h-NiO/In_2O_3 sensors was significantly higher than the other two sensors, implying that the gas response of In_2O_3 sensors was tightly dependent upon the configuration of the NiO component. Longer reaction time of hydrothermal reaction generated more NiO content. The enrichment of NiO nanoparticles on the surface of In_2O_3 displayed a better response.

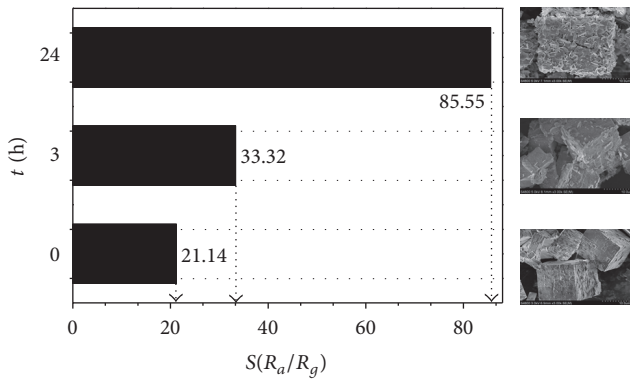

FIGURE 4: The sensitivity of pure In_2O_3 and NiO/In_2O_3 materials prepared by hydrothermal reaction for 3.0 h and 24.0 h, respectively, to 600 ppm methanal gas.

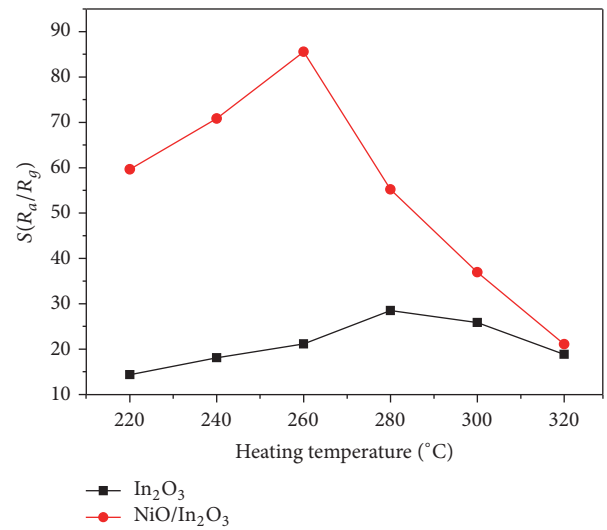

FIGURE 5: The sensitivity of pure In_2O_3 and NiO/In_2O_3 materials to 600 ppm methanal at different temperatures.

There were several probable reasons which might be responsible for the preferable gas sensing performance of the p-n heterojunction-like NiO/In_2O_3. (1) The NiO/In_2O_3 with higher specific surface area than In_2O_3 substrate could afford more active sites to react with methanal gas molecules [41]. (2) The p-n heterojunction-like NiO/In_2O_3 structure was favorable for preventing the undesirable aggregation and ensured the stability of the sensors. (3) It is deemed to be a hetero-p-n-junction between NiO and In_2O_3 that increased the sensor resistance. Therefore, NiO/In_2O_3 samples showed superior methanal sensor performance.

For the NiO/In_2O_3 sensors, working temperature is also an important factor. Figure 5 presents the relationship between the working temperature and the sensor response. In the range of 220–320°C, the sensor response to methanol was enhanced with increasing working temperature and up to 85.5 at 260°C. Later, the sensor response of NiO/In_2O_3 was decreased at higher working temperature. The optimum working temperature of NiO/In_2O_3 sensor device was determined at 260°C. As is well known, the increase of temperature would facilitate the chemical reaction and then promote the gas response. But further increase in temperature leads to the decrease of response. The reason is put down to the low utilization rate of the sensing layer because the gas is consumed at the surface of the sensing layer, leading to reduction of the penetration depth of the target gas [42]. Lower temperature might not excite the adsorbed methanal and free electrons in NiO/In_2O_3 effectively, while, at higher temperature, methanal gas molecules were hard to be adsorbed, and oxygen molecules might be also desorbed, causing less influence on the resistance of the film [43]. In the same measurement system, the response of pure In_2O_3 to 600 ppm methanal was 28.5 at 280°C, which was much lower than that of the p-n heterojunction-like NiO/In_2O_3. These findings showed that the p-n heterojunction-like gas sensor had achieved more superior sensing properties than that of bare In_2O_3 materials.

The response and recovery time, which were also important parameters for a gas sensor, were generally defined as the times to reach 90% variation in resistance upon exposure to methanal and air were defined as the 90% response time and 90% recovery time, respectively. And the faster the gas diffusion speed is, the less the response/recovery time is needed [44, 45]. In Figure 6, for 600 ppm methanal gas, NiO/In_2O_3 sensors exhibited rapid gas sensing behavior when the target gases were injected or released. These results could be attributed to the nanogaps between NiO and In_2O_3. Benefiting from the nanogaps between NiO and In_2O_3, which could improve the gas diffusion speed, the p-n heterojunction-like NiO/In_2O_3 sensors perform higher rates of gas adsorption and desorption than solo In_2O_3. For the response time, the NiO/In_2O_3 sensors exhibited a shorter response time for all the heating temperatures. After injection of methanal gas, a higher concentration of the adsorbed oxygen species on the surface of the composite microparticle sensor reacted with methanal, resulting in a short response time. Even though the recovery time of the composite microparticle sensor was shorter than that of the pristine In_2O_3 sensor, no significant optimizing effect was observed for the composites. The recovery reaction consists of the following serial steps: (1) gas-phase diffusion of oxygen to the sensor material surface, (2) adsorption of the oxygen molecules at the surface, (3) dissociation of oxygen molecules into oxygen atoms, and (4) ionization of the atomic oxygen. The slower recovery time might be due to the sluggish surface reactions, including the adsorption, dissociation, and ionization of oxygen, compared with the fast gas-phase diffusion in the present sensor [46].

Figure 7 shows the sensor responses of the sensor device upon exposure to various concentrations of methanal at a working temperature of 260°C. The sensitivities of pristine In_2O_3 and NiO/In_2O_3 materials were studied. The values of NiO/In_2O_3 sensitivity were observed to range from 31.78 to 213.18, whereas the sensitivity of pure In_2O_3 ranged from 26.58 to 73.78. The higher sensitivity of NiO/In_2O_3 towards the methanal samples compared to the parallel In_2O_3

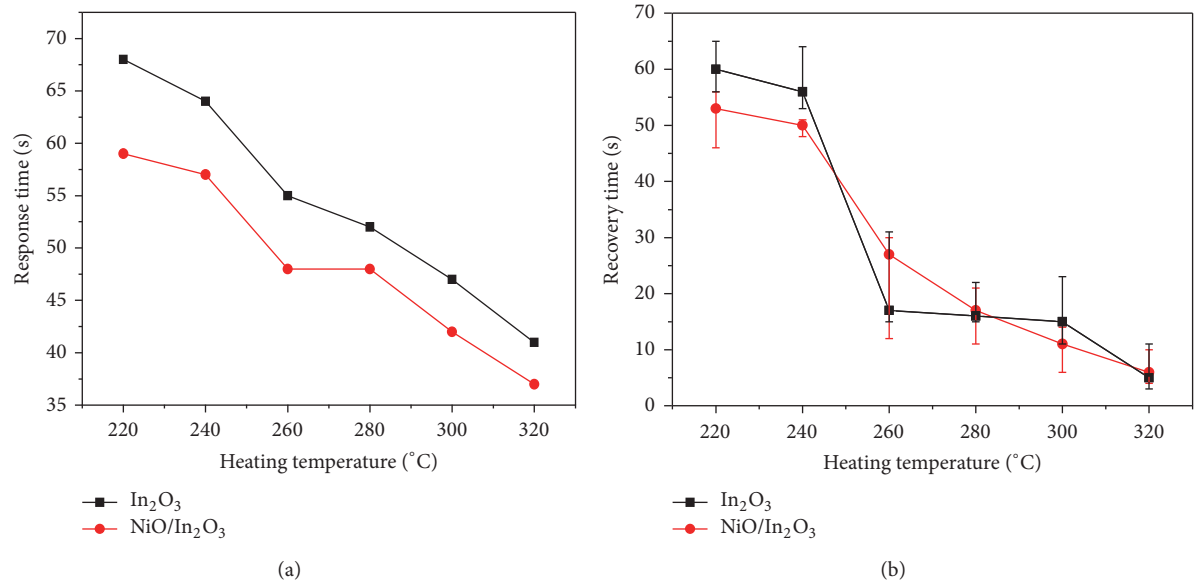

FIGURE 6: (a) The response time of pure In_2O_3 and NiO/In_2O_3 materials to 600 ppm methanal gas at different temperatures. (b) The recovery time of pure In_2O_3 and NiO/In_2O_3 materials to 600 ppm methanal gas at different temperatures.

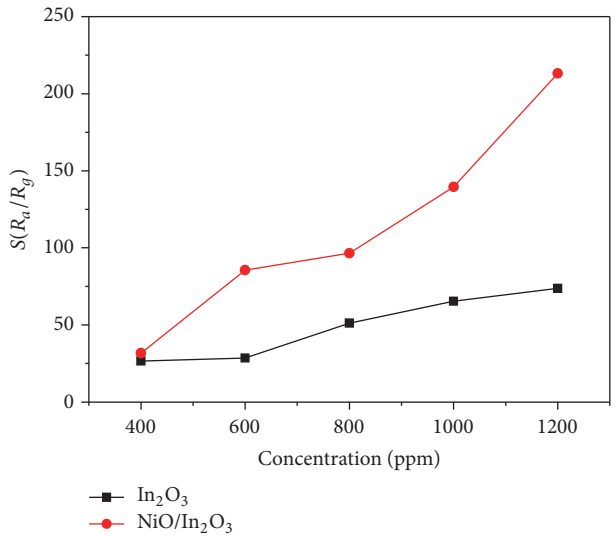

FIGURE 7: The sensitivity of pure In_2O_3 and NiO/In_2O_3 materials to different concentrations of methanal at 260°C.

substrate can be attributed to the improved surface area. The higher surface area of NiO/In_2O_3, arising after the NiO treatment of In_2O_3 (previously observed in the SEM images in Figure 1), provided a larger surface for the sorption process. Thereby, the response to methanal of p-n heterojunction-like NiO/In_2O_3 was better than that of the as-prepared pure In_2O_3 samples. Moreover, at a low concentration of 600 ppm of methanal, the relative response of NiO/In_2O_3 is about 31.8. When increasing the concentration of methanal, the response of the NiO/In_2O_3 also sharply increased. For the NiO/In_2O_3, the response to 1200 ppm methanal is up to 213.2, representing an almost threefold difference of sensitivity when compared to the pure In_2O_3 at the concentration of 1200 ppm of methanal. Simply, better sensitivity was expected to higher methanal concentration, which might be a result of fast diffusion and reaction rate of methanol with high concentration [47].

In an attempt to investigate the selective detection behavior of NiO/In_2O_3 sensors, the selectivity of samples against other interference gases was also discussed by measuring the response to 600 ppm methanal, ethanol, ammonia, benzene, toluene, and chloroform at 260°C (Figure 8). It can be seen that the NiO/In_2O_3 exceeded In_2O_3 responses for methanol and ethanol only while other gases are comparable and almost negligible. Such phenomenon demonstrated that methanal could be sensitively and selectively detected by employing NiO/In_2O_3 sensor.

In theory, the negatively charged oxygen has inherent ability to oxidize the reducing gas, generating electrons which decrease the hole concentration in the surface layer through the electron-hole recombination [48]. Therefore, the resistance of gas sensor is added upon exposure to a reducing gas. In the current work, the chemical mechanisms of NiO/In_2O_3 sensors to methanal can be shown in the following reactions. Ion-sorbed oxygen behaved as the electron extractor from the bulk NiO/In_2O_3 sensors, and the methanal molecules were postulated to be oxidized by the ion-sorbed oxygen (where O_2 was the oxygen in gas and O^- was ion-sorbed oxygen):

$$O_2 + e^- \longrightarrow 2O^- \quad (1)$$

$$HCHO + 2O^- \longrightarrow CO_2 + H_2O + e^- \quad (2)$$

Therefore, the electron extracted by oxygen came back to the bulk, and the resistance of the NiO/In_2O_3 sensors changed to generate a sensor signal. The proposed process of NiO/In_2O_3 and reaction mechanism of NiO/In_2O_3 sensors to methanal gas is shown in Figure 9.

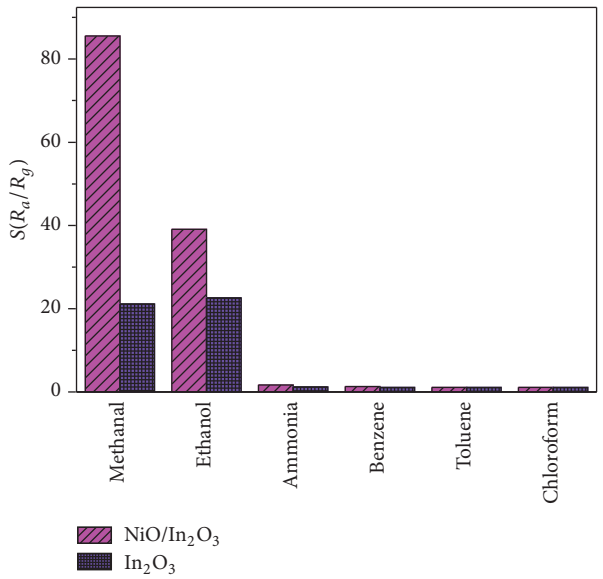

FIGURE 8: The sensitivity of pure In_2O_3 and NiO/In_2O_3 materials to 600 ppm different gases at 260°C.

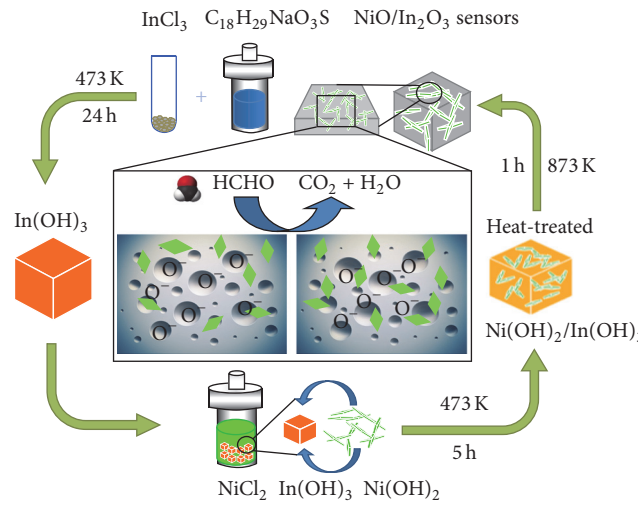

FIGURE 9: Schematic of the reaction mechanism of NiO/In_2O_3 sensors to methanal gas.

Note that when the background hole concentration was lower, the change of hole concentration had an increasing trend since the gas sensing reaction would result in a higher variation in sensor resistance. Similar results have been reported previously that both the gas response and sensor resistance of In_2O_3 were enhanced by doping with ZnO [49, 50]. Accordingly, in the case of p-n heterojunction-like NiO/In_2O_3 sensors, the enhancement of sensor resistance and gas response could be attributed to the lessened hole concentration due to NiO doping.

The prominent increasing of methanal gas response effectuated by decorating p-type NiO petals with n-type In_2O_3 could be explained by the formation of abundant p-n junctions. The hole accumulation layer for conduction would be narrowed by the hole depletion layer formation of the n-type In_2O_3 cubes, which offered an explanation for the superior resistance of the NiO/In_2O_3 sensors. It should be noted that W_n and W_p (the widths of the space charge layer of the n-oxide and p-oxide semiconductor sides, resp.) also relied on N_d/N_a (relative ratio of the charge carrier concentration, and N_d is donor density; N_a stands for acceptor density). The $W_n \cdot N_d = W_p \cdot N_a$ equation (given that the W_p value will go up as N_a reduces) meant that NiO/In_2O_3 not only declined the hole concentration within the hole accumulation layer but also gave rise to the hole depletion layer to be thicker. In turn, the p-conducting channel became narrow. Hereby, a small variation in charge carrier concentration could bring about higher change in sensor resistance.

4. Conclusions

In summary, a highly sensitive and selective methanal sensor was designed via coating the petal-shaped p-type NiO onto the surface of n-In_2O_3 cubes. The as-synthesized product was characterized using SEM-EDS, XRD, and FT-IR. The experimental results of detecting the gas response verified that the gas sensing characteristic of NiO/In_2O_3 sensors was significantly different from the pure In_2O_3 cubes. The gas response value of NiO/In_2O_3 sensors was 85.55 to 600 ppm methanal gas at 260°C, and this value was almost four times more than pure In_2O_3 substrate. The prominent increasing of methanal gas response effectuated by decorating p-type NiO petals with n-type In_2O_3 could be explained by the formation of abundant p-n junctions. The gas responses of NiO/In_2O_3 sensors to ammonia, benzene, toluene, and chloroform were extremely weak at the similar circumstance. Thus, a superior response, quick recovery, and higher selectivity of gas response to 600 ppm methanal were achieved by decorating In_2O_3 cubic particles with petal-shaped NiO nanoclusters. Such dual-role nature of decorating the NiO microparticles onto In_2O_3 cubes therefore provides a novel approach to designing highly sensitive, selective, and rapidly recovering gas sensors based on n-type oxide semiconductors.

Competing Interests

The authors declare that they have no potential or actual conflict of interests pertaining to this submission.

Acknowledgments

This work was supported by Research Project of Foundation of Shaanxi Provincial Department of Education (no. 14JK1657) and the Fundamental Research Funds for the Central Universities (no. 310829161015 and no. 310829162014).

References

[1] A. J. Paine and A. D. Dayan, "Defining a tolerable concentration of methanol in alcoholic drinks," *Human and Experimental Toxicology*, vol. 20, no. 11, pp. 563–568, 2001.

[2] H. L. C. Pinheiro, M. V. De Andrade, P. A. D. P. Pereira, and J. B. De Andrade, "Spectrofluorimetric determination of formaldehyde in air after collection onto silica cartridges coated with Fluoral P," *Microchemical Journal*, vol. 78, no. 1, pp. 15–20, 2004.

[3] V. Sibirny, O. Demkiv, H. Klepach, T. Honchar, and M. Gonchar, "Alcohol oxidase- and formaldehyde dehydrogenase-based enzymatic methods for formaldehyde assay in fish food products," *Food Chemistry*, vol. 127, no. 2, pp. 774–779, 2011.

[4] A. Allouch, M. Guglielmino, P. Bernhardt, C. A. Serra, and S. Le Calvé, "Transportable, fast and high sensitive near real-time analyzers: formaldehyde detection," *Sensors and Actuators, B: Chemical*, vol. 181, pp. 551–558, 2013.

[5] H. Wang, J. Ding, X. Du et al., "Determination of formaldehyde in fruit juice based on magnetic strong cation-exchange resin modified with 2,4-dinitrophenylhydrazine," *Food Chemistry*, vol. 131, no. 1, pp. 380–385, 2012.

[6] S. N. Azizi, S. Ghasemi, and F. Amiripour, "Nickel/P nanozeolite modified electrode: a new sensor for the detection of formaldehyde," *Sensors and Actuators, B: Chemical*, vol. 227, pp. 1–10, 2016.

[7] Y. Li, J. Xu, J. Chao et al., "High-aspect-ratio single-crystalline porous In_2O_3 nanobelts with enhanced gas sensing properties," *Journal of Materials Chemistry*, vol. 21, no. 34, pp. 12852–12857, 2011.

[8] M. M. Arafat, A. S. M. A. Haseeb, and S. A. Akbar, "A selective ultrahigh responding high temperature ethanol sensor using TiO_2 nanoparticles," *Sensors*, vol. 14, no. 8, pp. 13613–13627, 2014.

[9] L. Han, D. J. Wang, J. B. Cui, L. P. Chen, T. F. Jiang, and Y. H. Lin, "Study on formaldehyde gas-sensing of In_2O_3-sensitized ZnO nanoflowers under visible light irradiation at room temperature," *Journal of Materials Chemistry*, vol. 22, no. 25, pp. 12915–12920, 2012.

[10] A. Kolmakov and M. Moskovits, "Chemical sensing and catalysis by one-dimensional metal-oxide nanostructures," *Annual Review of Materials Research*, vol. 34, pp. 151–180, 2004.

[11] T. T. Wang, S. Y. Ma, L. Cheng et al., "Facile fabrication of multishelled SnO_2 hollow microspheres for gas sensing application," *Materials Letters*, vol. 164, pp. 56–59, 2016.

[12] N. D. Hoa, V. V. Quang, D. Kim, and N. V. Hieu, "General and scalable route to synthesize nanowire-structured semiconducting metal oxides for gas-sensor applications," *Journal of Alloys and Compounds*, vol. 549, pp. 260–268, 2013.

[13] N. Barsan, C. Simion, T. Heine, S. Pokhrel, and U. Weimar, "Modeling of sensing and transduction for p-type semiconducting metal oxide based gas sensors," *Journal of Electroceramics*, vol. 25, no. 1, pp. 11–19, 2010.

[14] Y. Wang, J.-L. Cao, M.-G. Yu et al., "Porous α-Fe_2O_3 hollow microspheres: hydrothermal synthesis and their application in ethanol sensors," *Materials Letters*, vol. 100, pp. 102–105, 2013.

[15] X. Chen, Y. Wang, J. Guo, J. Jian, L. Gu, and Z. Zhang, "In-situ potential mapping of space charge layer in GaN nanowires under electrical field by off-axis electron holography," *Progress in Natural Science: Materials International*, vol. 26, no. 2, pp. 163–168, 2016.

[16] A. M. Cowley, "Depletion capacitance and diffusion potential of gallium phosphide Schottky-Barrier diodes," *Journal of Applied Physics*, vol. 37, no. 8, pp. 3024–3032, 1966.

[17] I.-D. Kim, A. Rothschild, and H. L. Tuller, "Advances and new directions in gas-sensing devices," *Acta Materialia*, vol. 61, no. 3, pp. 974–1000, 2013.

[18] H.-J. Kim and J.-H. Lee, "Highly sensitive and selective gas sensors using p-type oxide semiconductors: overview," *Sensors and Actuators, B: Chemical*, vol. 192, pp. 607–627, 2014.

[19] M. Hübner, C. E. Simion, A. Tomescu-Stănoiu, S. Pokhrel, N. Bârsan, and U. Weimar, "Influence of humidity on CO sensing with p-type CuO thick film gas sensors," *Sensors and Actuators B: Chemical*, vol. 153, no. 2, pp. 347–353, 2011.

[20] S. S. Kaye and J. R. Long, "Hydrogen storage in the dehydrated prussian blue analogues $M_3[Co(CN)_6]_2$ (M = Mn, Fe, Co, Ni, Cu, Zn)," *Journal of the American Chemical Society*, vol. 127, no. 18, pp. 6506–6507, 2005.

[21] S. Chen, W. Zhao, W. Liu, and S. Zhang, "Preparation, characterization and activity evaluation of p–n junction photocatalyst p-ZnO/n-TiO_2," *Applied Surface Science*, vol. 255, no. 5, pp. 2478–2484, 2008.

[22] C. Shifu, C. Lei, G. Shen, and C. Gengyu, "The preparation of coupled WO_3/TiO_2 photocatalyst by ball milling," *Powder Technology*, vol. 160, no. 3, pp. 198–202, 2005.

[23] C. Shifu, Z. Sujuan, L. Wei, and Z. Wei, "Preparation and activity evaluation of p-n junction photocatalyst NiO/TiO_2," *Journal of Hazardous Materials*, vol. 155, no. 1-2, pp. 320–326, 2008.

[24] L. Wei, C. Shifu, Z. Sujuan, Z. Wei, Z. Huaye, and Y. Xiaoling, "Preparation and characterization of *p–n* heterojunction photocatalyst *p*-$CuBi_2O_4$/n-TiO_2 with high photocatalytic activity under visible and UV light irradiation," *Journal of Nanoparticle Research*, vol. 12, no. 4, pp. 1355–1366, 2010.

[25] Z. Y. Wang, B. B. Huang, Y. Dai et al., "Highly photocatalytic ZnO/In_2O_3 heteronanostructures synthesized by a coprecipitation method," *Journal of Physical Chemistry C*, vol. 113, no. 11, pp. 4612–4617, 2009.

[26] W. Zang, Y. Nie, D. Zhu, P. Deng, L. Xing, and X. Xue, "Core-shell In_2O_3/ZnO nanoarray nanogenerator as a self-powered active gas sensor with high H_2S sensitivity and selectivity at room temperature," *Journal of Physical Chemistry C*, vol. 118, no. 17, pp. 9209–9216, 2014.

[27] J. Wang, X. Gan, Z. Li, and K. Zhou, "Microstructure and gas sensing property of porous spherical In_2O_3 particles prepared by hydrothermal method," *Powder Technology*, vol. 303, pp. 138–146, 2016.

[28] X. Lu, L. Zhang, H. Zhao, K. Yan, Y. Cao, and L. Meng, "Synthesis, characterization and gas sensing properties of $In(OH)_3$ and In_2O_3 nanorods through carbon spheres template method," *Journal of Materials Science and Technology*, vol. 28, no. 5, pp. 396–400, 2012.

[29] H. H. Liu, F. D. Qu, H. Gong, H. Jiang, and M. H. Yang, "Template-free synthesis of In_2O_3 nanoparticles and their acetone sensing properties," *Materials Letters*, vol. 182, pp. 340–343, 2016.

[30] X. Sun, H. Hao, H. Ji, X. Li, S. Cai, and C. Zheng, "Nanocasting synthesis of In_2O_3 with appropriate mesostructured ordering and enhanced gas-sensing property," *ACS Applied Materials and Interfaces*, vol. 6, no. 1, pp. 401–409, 2014.

[31] X. Wang, J. Zhang, L. Wang et al., "High response gas sensors for formaldehyde based on Er-doped In_2O_3 nanotubes," *Journal of Materials Science and Technology*, vol. 31, no. 12, pp. 1175–1180, 2015.

[32] G. Mattei, P. Mazzoldi, M. L. Post, D. Buso, M. Guglielmi, and A. Martucci, "Cookie-like Au/NiO nanoparticles with optical gas-sensing properties," *Advanced Materials*, vol. 19, no. 4, pp. 561–564, 2007.

[33] T. S. Mintz, Y. V. Bhargava, S. A. Thorne et al., "Electrochemical synthesis of functionalized nickel oxide nanowires," *Electrochemical and Solid-State Letters*, vol. 8, no. 9, pp. D26–D30, 2005.

[34] C. Tongxiang, Z. Yanwei, Z. Wei, G. Cuijing, and Y. Xiaowei, "Synthesis of nanocomposite nickel oxide/yttrium-stabilized zirconia (NiO/YSZ) powders for anodes of solid oxide fuel cells (SOFCs) via microwave-assisted complex-gel autocombustion," *Journal of Power Sources*, vol. 195, no. 5, pp. 1308–1315, 2010.

[35] N. Li, E. A. Gibson, P. Qin et al., "Double-layered NiO photocathodes for p-type DSSCs with record IPCE," *Advanced Materials*, vol. 22, no. 15, pp. 1759–1762, 2010.

[36] D. Ju, H. Xu, Q. Xu et al., "High triethylamine-sensing properties of NiO/SnO_2 hollow sphere P–N heterojunction sensors," *Sensors and Actuators, B: Chemical*, vol. 215, pp. 39–44, 2015.

[37] Y.-R. Li, C.-Y. Wan, C.-T. Chang et al., "Thickness effect of NiO on the performance of ultraviolet sensors with p-NiO/n-ZnO nanowire heterojunction structure," *Vacuum*, vol. 118, pp. 48–54, 2015.

[38] B.-H. Liu, S.-H. Yu, S.-F. Chen, and C.-Y. Wu, "Hexamethylenetetramine directed synthesis and properties of a new family of α-nickel hydroxide organic-inorganic hybrid materials with high chemical stability," *Journal of Physical Chemistry B*, vol. 110, no. 9, pp. 4039–4046, 2006.

[39] D. Chen and L. Gao, "A new and facile route to ultrafine nanowires, superthin flakes and uniform nanodisks of nickel hydroxide," *Chemical Physics Letters*, vol. 405, no. 1–3, pp. 159–164, 2005.

[40] P. Sun, X. Zhou, C. Wang, K. Shimanoe, G. Y. Lu, and N. Yamazoe, "Hollow SnO_2/α–Fe_2O_3 spheres with a double-shell structure for gas sensors," *Journal of Materials Chemistry A*, vol. 2, no. 5, pp. 1302–1308, 2014.

[41] J. Sun, J. Cheng, C. Wang, X. Ma, M. Li, and L. Yuan, "Synthesis and morphological control of nickel hydroxide for lithium-nickel composite oxide cathode materials by an eddy circulating precipitation method," *Industrial and Engineering Chemistry Research*, vol. 45, no. 6, pp. 2146–2149, 2006.

[42] F. Fang, L. Bai, H. Sun et al., "Hierarchically porous indium oxide nanolamellas with ten-parts-per-billion-level formaldehyde-sensing performance," *Sensors and Actuators, B: Chemical*, vol. 206, pp. 714–720, 2015.

[43] N. Han, Y. Tian, X. Wu, and Y. Chen, "Improving humidity selectivity in formaldehyde gas sensing by a two-sensor array made of Ga-doped ZnO," *Sensors and Actuators B: Chemical*, vol. 138, no. 1, pp. 228–235, 2009.

[44] X. Tong, Y. Qin, X. Guo et al., "Enhanced catalytic activity for methanol electro-oxidation of uniformly dispersed nickel oxide nanoparticles-carbon nanotube hybrid materials," *Small*, vol. 8, no. 22, pp. 3390–3395, 2012.

[45] C. Ge, C. Xie, D. Zeng, and S. Cai, "Formaldehyde-, benzene-, and xylene-sensing characterizations of Zn–W–O nanocomposite ceramics," *Journal of the American Ceramic Society*, vol. 90, no. 10, pp. 3263–3267, 2007.

[46] T. Chen, Q. J. Liu, Z. L. Zhou, and Y. D. Wang, "The fabrication and gas-sensing characteristics of the formaldehyde gas sensors with high sensitivity," *Sensors and Actuators B: Chemical*, vol. 131, no. 1, pp. 301–305, 2008.

[47] J. R. Huang, K. Yu, C. P. Gu et al., "Preparation of porous flower-shaped SnO_2 nanostructures and their gas-sensing property," *Sensors and Actuators B: Chemical*, vol. 147, no. 2, pp. 467–474, 2010.

[48] H.-J. Kim, H.-M. Jeong, T.-H. Kim, J.-H. Chung, Y. C. Kang, and J.-H. Lee, "Enhanced ethanol sensing characteristics of In_2O_3-decorated NiO hollow nanostructures via modulation of hole accumulation layers," *ACS Applied Materials and Interfaces*, vol. 6, no. 20, pp. 18197–18204, 2014.

[49] F. Fang, L. Bai, D. Song et al., "Ag-modified In_2O_3/ZnO nanobundles with high formaldehyde gas-sensing performance," *Sensors (Switzerland)*, vol. 15, no. 8, pp. 20086–20096, 2015.

[50] B. Huang, C. Zhao, M. Zhang et al., "Doping effect of In_2O_3 on structural and ethanol-sensing characteristics of ZnO nanotubes fabricated by electrospinning," *Applied Surface Science*, vol. 349, pp. 615–621, 2015.